JOURNAL OF AIRCRAFT
Vol. 38, No. 4, July–August 2001

Engineering Notes

ENGINEERING NOTES are short manuscripts describing new developments or important results of a preliminary nature. These Notes cannot exceed 6 manuscript pages and 3 figures; a page of text may be substituted for a figure and vice versa. After informal review by the editors, they may be published within a few months of the date of receipt. Style requirements are the same as for regular contributions (see inside back cover).

Computational Study of the High-Lift A-Airfoil

Adam Jirásek*
Aeronautical Research and Test Institute, 199 00 Prague, Czech Republic
and
Peter Eliasson† and Stefan Wallin‡
Swedish Defence Research Agency, SE-17290 Stockholm, Sweden

Introduction

ACCURATE prediction of the aerodynamic features of airfoils and wings as well as complete aircraft configurations are important challenges. One important problem is the prediction of high-lift configurations and especially the prediction of stall. These cases include phenomena like transition to turbulence, boundary-layer separation, free shear layers in the wake, adverse pressure gradients, surface curvature, etc. Vast amount of effort has been put into this aerodynamic problem including testing of different numerical schemes, grid-dependence studies, and in particular turbulence modeling. However, unanswered questions still remain concerning the importance of the grid topology and its quality, numerical scheme, and the interdependence of these factors. These questions need to be answered before any definite conclusion concerning the modeling of the turbulence can be made.

This article deals with numerical computations of the A-airfoil test case[1] at the angle of attack of 13.3 deg. The Mach number is 0.15, and the Reynolds number is 2.07×10^6 with respect to the chord length. The wind-tunnel model has a trailing-edge thickness of 0.5% of the chord, which has been neglected in most previous computations where the geometry was modified to have a sharp trailing edge. As noted by Jeffrey and Zhang,[2] Stanaway et al.,[3] Thompson and Whitelaw,[4] and Thompson and Lotz,[5] the shape of the trailing edge could have a big influence on the characteristics of the profile particularly at high angle of attack where separation of the boundary layer occurs.

Previous works (see Haase et al.[1] and Lorentzen and Lindblad[6]) were focusing mainly on the different turbulence models. It was found by Lorentzen and Lindblad[6] that the separated boundary layer reattaches at the very end of the trailing edge. It was discussed that this effect could be connected with either numerical or physical problems caused by the sharp trailing edge of the profile geometry and the C grid topology. In this study the focus will be to assess the importance of a blunt trailing edge and the quality of the grid in that region.

Computational Results

The Reynolds-averaged Navier–Stokes equations were solved by using the finite volume code EURANUS[7] for structured multiblock grids. Convergence to steady state is obtained by explicit local time stepping and multigrid acceleration. To improve the convergence, a local low-speed preconditioner (see Person[8] and Turkel et al.[9]) of Turkel's type has been used. When solving time-dependent problems, a second-order accurate implicit approach was used using the dual time-stepping procedure proposed by Jameson.[10]

At the far field a Riemann boundary condition corrected with lift-induced circulation is used (see Lorentzen and Lindblad[6]) and the turbulent kinetic energy and specific rate of dissipation were prescribed to $k = 1\ \mathrm{m^2\ s^{-2}}$ and $\omega = 11{,}111\ \mathrm{s^{-1}}$, respectively. Transition to turbulence was prescribed at 30% of the chord at the pressure side and 12% at the suction side.

To evaluate the influence of the trailing-edge geometry and of the grid quality around the trailing edge on the solution two different grids, C and C–H–O, were constructed. The C grid has a sharp trailing edge and a standard one-block C topology with 66,000 grid points. The C–H–O grid resolves the blunt trailing edge by using a local near-wall O topology and uses 65,000 grid points. The details of the grid around the trailing edge are shown in Fig. 1. A set of coarser grids, C2 and C2–H2–O2, were constructed by removing every second grid point in all directions.

The standard explicit local time-stepping method for obtaining a steady-state solution did not converge completely for the blunt trailing edge. However, when switching to the much more computer expensive time-accurate integration method a steady-state solution was obtained. The unsteadiness resulting from the local time stepping is, thus, only a numerical anomaly. All computational results on the C–H–O grid are obtained using the time-accurate implicit integration method.

The comparisons between the different grids were carried out using the Wallin and Johansson[11] EARSM k–ω turbulence model. Drag was calculated by integrating the momentum losses in the wake behind the profile using the method of Young.[12]

Trailing-Edge Bluntness

The influence of the bluntness of the trailing edge is assessed by comparing the computational results on the C and C–H–O grids.

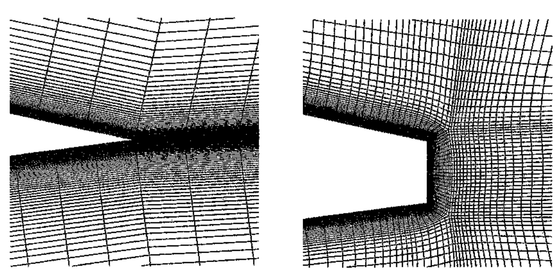

Fig. 1 Computational grid around the A-airfoil trailing edge: a) one-block C grid and b) three-block C–H–O grid. $0.99 \leq x \leq 1.01$, $-0.022 \leq y \leq -0.002$.

Received 8 December 2000; revision received 8 April 2001; accepted for publication 29 April 2001.

*Research Engineer, Beranových 130; vzlu_pal@mbox.vol.cz.
†Senior Research Engineer, Aeronautics Division, FFA; peter.eliasson@foi.se. Member AIAA.
‡Senior Research Engineer, Aeronautics Division, FFA; stefan.wallin@foi.se. Member AIAA.

Table 1 Lift, drag, and separation point at different grids for the A-airfoil (Turbulence is modeled using EARSM)

Grid	C	C2	C–H–O	C2–H2–O2	Experiment
c_L	1.550	1.542	1.601	1.579	1.562
c_D	0.0198	——	0.0206	0.0287	0.0208
Separation	90.2%	89.3%	91.7%	87.3%	82%

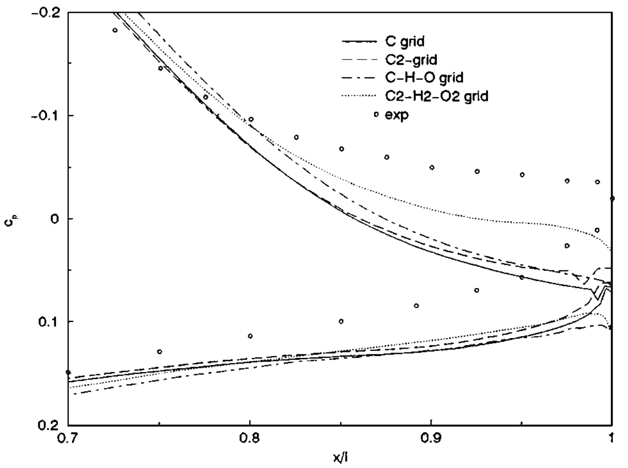

a)

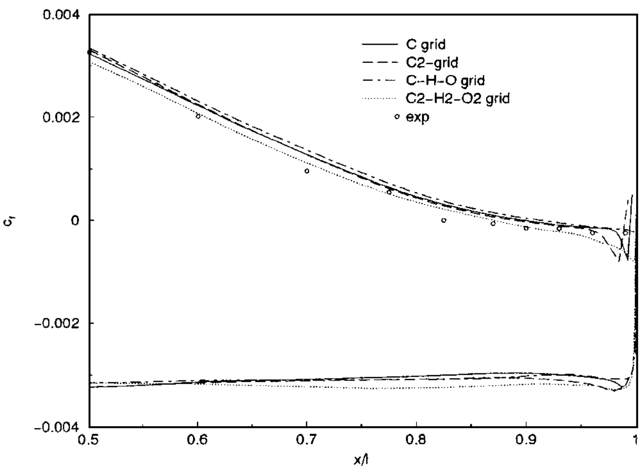

b)

Fig. 2 Coefficients a) c_p and b) c_f at different grids for the A-airfoil. Turbulence is modeled using EARSM.

A significant higher lift c_L is obtained from the C–H–O grid (see Table 1), but only a minor influence on the drag c_D and separation point can be observed. The increased lift is also noted in a decreased pressure coefficient c_p near the trailing edge on the suction side for the blunt trailing-edge case (see Fig. 2a). No significant difference in skin-friction coefficient c_f in Fig. 2b can be seen.

The main explanation for the increased lift is that the separation point (Rotta condition) is located at the lower edge of the blunt trailing edge compared to the sharp trailing edge where the separation point should be at the trailing edge. As noted in Jeffrey and Zhang,[2] the vortices developing behind the trailing edge give rise to trailing-edge suction and cause increased lift.

Actually, in the computation of the sharp trailing edge the separation point is located a few grid points upstream of the trailing edge on the suction side, which can be seen as a wiggle in c_f close to the trailing edge in Fig. 2b. The reason for that is the artificial numerical singularity at the trailing edge, and it leads to an even more decreased lift.

The velocity profiles at the positions of 96 and 99% of the chord on the suction side (see Fig. 3) show that the computation on the

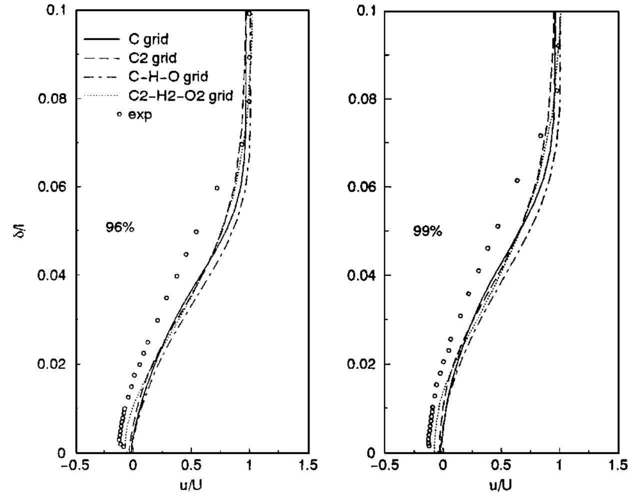

Fig. 3 Velocity profiles at different grids for the A-airfoil at 96 and 99% of cord. Turbulence is modeled using EARSM.

C–H–O grid gives a somewhat thinner boundary layer than that obtained on the C grid. The wiggle in c_f close to the trailing edge can only be seen as a small near-wall disturbance in the velocity profile at 99%.

The presence of the blunt trailing edge effectively enhances the spreading of the near wake and influences the flow close to the leading edge as well as the global lift. By approximating the trailing edge as sharp, which is usually done in computational fluid dynamics (CFD) computations, these effects are lost in the computations. Moreover, when including the blunt trailing edge in the computational grid the base region must be properly resolved by using a local O topology in order to capture the enhanced spreading and the shifted position of the separation point caused by the bluntness (see Jirásek et al.[13] for more details).

Grid Convergence

The computations on the coarser grids, C2 and C2–H2–O2 where every second grid point has been removed, are used for assessing the level of grid convergence. There is a significant difference in drag and in the local pressure distribution close to the trailing edge between the two grid levels. Also the separation position is affected. However, the solutions are reasonably well resolved also at the coarser level giving only minor differences in the solution away from the details around the trailing edge. Thus, the solution on the fine grids are assumed to be almost grid converged, and the differences between the different aspects of geometry and modeling are significant compared to the numerical error.

The solutions on the coarse grids in some aspects are closer to the experimental results compared to the fine grids. There are, however, a number of other factors than the grid convergence that influence the comparison with the experimental data. In particular the modeling of the turbulence is known to have a large influence on the solution. It is of major importance that a grid converged solution can be demonstrated before any comparison with experimental data is made.

The numerical method used is basically compressible, and low-speed preconditioning is used for speeding up the convergence to steady state. The Turkel[9] method does not only improve the steady-state convergence, but also the numerical or artificial dissipation for low-Mach-number cases. Without such preconditioning it is usually not possible to converge at an incompressible solution by letting the Mach number approach zero (see Turkel[9]). For this particular case the preconditioning improved also the grid-convergence rate. The differences between the different grid levels were much larger without preconditioning, e.g., the difference in the c_f peak after transition between the C and C2 grids were about seven times larger without preconditioning compared to the difference when preconditioning was used (see Jirásek et al.[13]).

Turbulence Modeling

Three different two-equation turbulence models were used in this study. The Menter[14] BSL and SST k–ω models and the Wallin and Johansson[11] explicit algebraic Reynolds-stress model (EARSM). The EARSM is based on the Menter BSL k–ω model where the original eddy-viscosity assumption is replaced with the algebraic Reynolds-stress relation. The computational results were obtained on the C–H–O grid.

The difference between the baseline (BSL) and shear-stress transport (SST) models is that the SST model has an empirical limitation of the eddy viscosity in cases with high shear rate. That limitation was found to improve the predicted forces and flowfield (see Table 2 and Figs. 4–7). A further improvement was obtained using the EARSM, where the eddy-viscosity assumption is completely avoided.

Even if there are significant improvements by using the more advanced EARSM, the separation is still predicted too short and, especially, too thin. Even at a position upstream of the separation at

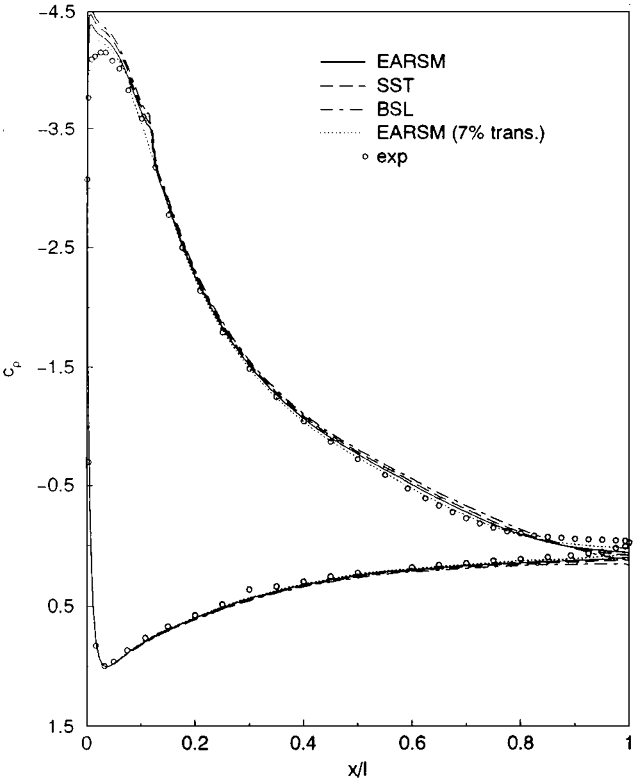

Fig. 4 c_p **coefficient for the A-airfoil at the C– H– O grid using different turbulence models.**

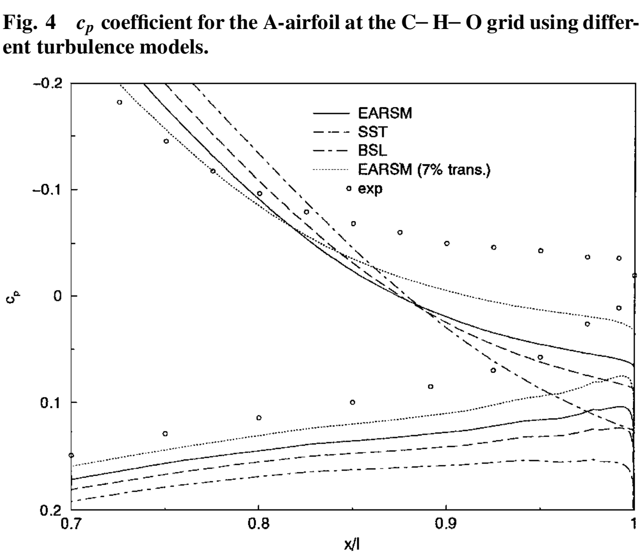

Fig. 5 Details of Fig. 4 around trailing edge.

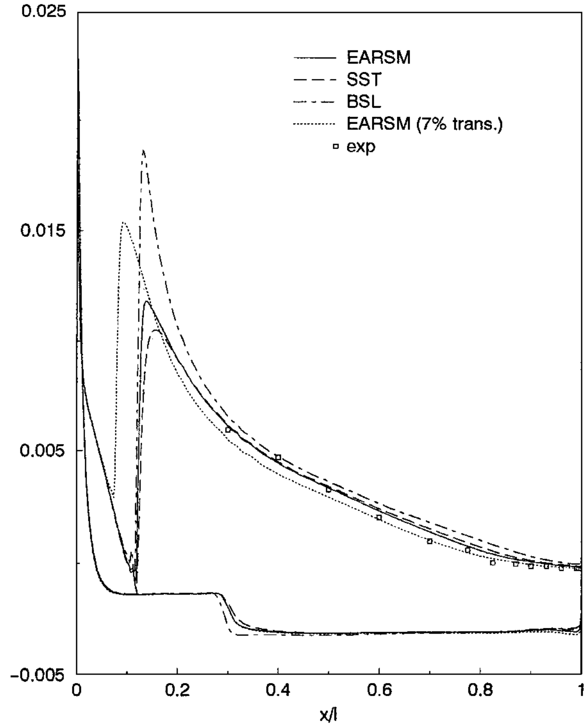

Fig. 6 c_f **coefficient for the A-airfoil at the C– H– O grid using different turbulence models.**

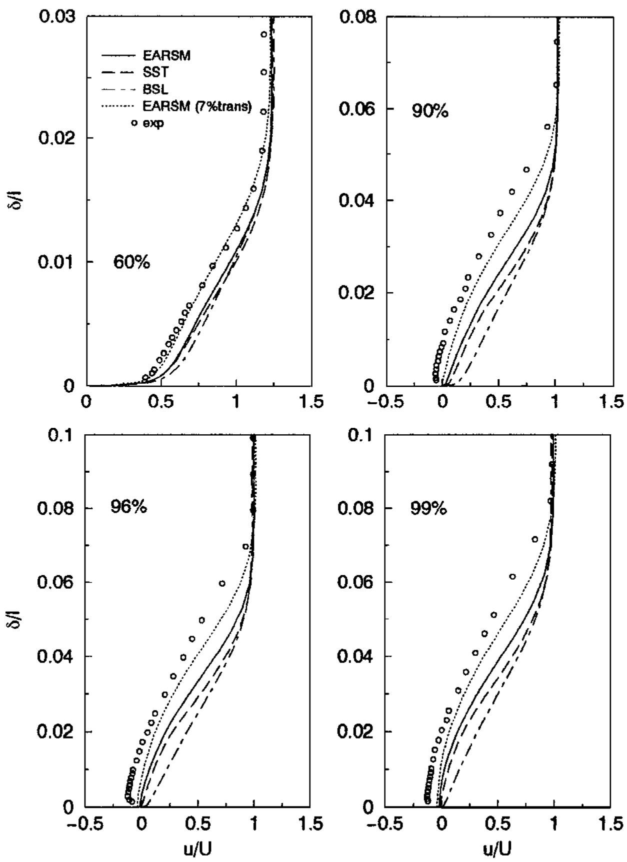

Fig. 7 Velocity profiles for the A-airfoil at the C– H– O grid using different turbulence models at 60, 90, 96, and 99% of cord.

Table 2 Lift, drag, and separation point for the A-airfoil at the C– H– O grid using different turbulence models

Model	BSL	SST	EARSM	EARSM (transition 7.8%)	Experiment
c_L	1.668	1.631	1.601	1.556	1.56
c_D	0.0202	0.0200	0.0206	0.0242	0.0208
Separation	96.6%	93.2%	91.7%	88.0%	82%

60% chord, the predicted velocity profiles are too full. The effect of the transition on the suction side is tested by moving the transition point 4% upstream using EARSM, which improved some aspects of the solution. The velocity profile at 60% chord in Fig. 7 is now better predicted, and the separation is increased leading to a better predicted lift. However, the drag is now overpredicted, and the laminar separation bubble has disappeared. Moreover, there is no support from the experimental data for moving the transition point upstream.

Conclusions

Almost grid-converged computational solutions on the A-profile has been demonstrated for both sharp and blunt trailing edges. Low-speed preconditioning improved the convergence to steady state as well as the grid convergence. The wind-tunnel profile has a trailing-edge bluntness of 0.5% of the chord, whereas most computations are made on a modified sharp trailing-edge geometry. It was found that the bluntness increases the lift by approximately 3% in the computations.

Three different two-equation turbulence models were tested. It was found that the more advanced algebraic Reynolds-stress model gave better predictions than more standard eddy-viscosity models. The lift and drag was fairly well predicted, but the trailing-edge separation was underestimated in length and especially in thickness.

Acknowledgment

This work was funded by the Aeronautical Research Institute of Sweden, FFA. The authors would like to express their thanks to Ingemar Lindblad for supervising this project. The first author would like to thank FFA for its financial support during his stay at FFA.

References

[1]Haase W., Chaput, E., Elsholz, E., Leschziner, M., and Mueller, V. R., "ECARP—European Computational Aerodynamics Research Projects: Validation of CFD Codes and Assessment of Turbulence Models," *Notes on Numerical Fluid Mechanics*, Vol. 58, Vieweg, Brunswich, Germany, 1997.

[2]Jeffrey, D., and Zhang, X., "Aerodynamics of Gourney Flaps on a Single-Element High-Lift Wing," *Journal of Aircraft*, Vol. 37, No. 2, 2000, pp. 295–301.

[3]Stanaway, S. K., McCroskey, W. J., and Kroo, I. M., "Navier–Stokes Analysis of Blunt Trailing Edge Airfoils," AIAA Paper 92-0024, Jan. 1992.

[4]Thompson, B. E., and Whitelaw, J. H., "Trailing-Edge Region of Airfoils," *Journal of Aircraft*, Vol. 26, No. 3, 1989, pp. 225–234.

[5]Thompson, B. E., and Lotz, D. R., "Divergent-Trailing-Edge Airfoil Flow," *Journal of Aircraft*, Vol. 33, No. 5, 1996, pp. 950–955.

[6]Lorentzen, L., and Lindblad, I. A. A., "Application of Two-Equation and EARSM Turbulence Models to High Lift Aerodynamics," AIAA Paper 99-3181, June–July 1999.

[7]Rizzi, A., Eliasson, P., Lindblad, I., Hirsch, C., and Lacor, C., "The Engineering of Multi-Block/Multigrid Software for Navier–Stokes Flow on Structured Meshes," *Computers and Fluids Journals*, Vol. 22, No. 2/3, 1993, pp. 341–367.

[8]Person, G., "Preconditioning for Low Mach Numbers in EURANUS," Aeronautical Research Inst. of Sweden, TN 1998-67, Stockholm, Nov. 1998.

[9]Turkel, E., Vatsa, V. N., and Radespiel, R., "Preconditioning Methods for Low-Speed Flows," NASA CR-201605, Inst. for Computer Applications in Science and Engineering, Rept. 96-57, Oct. 1996.

[10]Jameson, A., "Time Dependent Calculation Using Multigrid with Application to Unsteady Flows Past Airfoils and Wings," AIAA Paper 91-1596, June 1991.

[11]Wallin, S., and Johansson, A. V., "An Explicit Algebraic Reynolds Stress Model for Incompressible and Compressible Turbulent Flows," *Journal of Fluid Mechanics*, Vol. 403, Jan. 2000, pp. 89–132.

[12]Young, A. D., "Note on the Effect of Compressibility on Jone's Momentum Method of Measuring Profile Drag," Aeronautical Research Council, M 1881, 1939.

[13]Jirásek, A., Eliasson, P., and Wallin, S., "Computational Study of the High-Lift A-Airfoil," AIAA Paper 2001-0708, Jan. 2001.

[14]Menter, F. R., "Zonal Two Equation k–ω Turbulence Models for Aerodynamic Flows," AIAA Paper 93-2906, July 1993.

Improving the Convergence of the Doublet-Lattice Method Through Tip Corrections

Myles L. Baker*
The Boeing Company, Long Beach, California 90807-5608
and
William P. Rodden†
William P. Rodden, Ph.D., Inc., La Canada Flintridge, California 92011-2831

Introduction

FOLLOWING a suggestion of Rubbert[1] that when using the vortex lattice lifting surface method (VLM) equally spaced divisions should be inset from the tip by a fraction d $(0 < d < 1)$ of the strip width, Hough[2,3] has demonstrated impressive improvement in the estimation of lift curve slope $C_{L\alpha}$ of a wing without using an inordinate number of spanwise strips, specifically for $d = \frac{1}{4}$. The tip inset concept and some of Hough's convergence results for $C_{L\alpha}$ are shown in Fig. 1.

Hough's recommendation of $d = \frac{1}{4}$ was based on an analysis of an elliptical lift distribution, which is typical of a steady symmetrical aerodynamic loading. It is the purpose of this Note to investigate the convergence improvement that can be obtained by applying the tip inset correction to the oscillatory doublet-lattice method[4,5] (DLM, which reduces to the VLM in the steady case) for conditions in which elliptical lift distributions are not expected.

The tip correction is implemented by reducing the effective span of the wing (the span that is actually paneled with doublet-lattice boxes) by the factor NS/(NS + d), where NS is the number of spanwise strips and d is the tip inset factor (typically $\frac{1}{4}$). The lack of an aerodynamic panel on the most outboard tip of the wing has the effect of driving the tip loading toward the correct value of zero. Because the DLM assumes constant loading (spanwise) within a box, it requires a very high resolution to capture the correct wing-tip load distribution, and the DLM will typically overestimate the tip loading and approach the correct results from above as the resolution is refined.

Results

Rectangular Wings

Two wings pitching about their midchords at a Mach number of $M = 0.80$ are studied. The first wing has aspect ratio of $AR = 2$. It is divided into various NS and various numbers of chordwise boxes (NC) such that the maximum box aspect ratio is less than 8.0. The value of NC necessary for convergence depends on the reduced frequency $k_r = \omega c/2V$, where ω is the angular frequency (rad/sec), c is the reference chord ($c = 1.0$ for the rectangular wings), and V is the freestream velocity. The guideline of Ref. 5 recommends 50 boxes per wavelength λ, where $\lambda = \pi c/k_r$.

Received 1 February 2000; revision received 25 January 2001; accepted for publication 27 January 2001.

*Manager, Loads and Dynamics; myles.l.baker@boeing.com. Member AIAA.

†Consulting Engineer; billrodden@aol.com.